Supplementary Material

Rational Construction of a WS_2/CoS_2 Heterostructure Electrocatalyst for Efficient Hydrogen Evolution at All pH Values

Jun Wu[†,⊥], Tian Chen[†,⊥], Chenyu Zhu[‡], Junjie Du[‡], Longsheng Huang[§], Jing Yan[‖], Dongming Cai[§], Cao Guan[*,‡], and Chunxu Pan[*,†].

[†]School of Physics and Technology, and MOE Key Laboratory of Artificial Micro- and Nano-structures, Wuhan University, 299 Ba Yi Road, Wuhan 430072, P.R. China.

[‡]Institute of Flexible Electronics, Xi'an Institute of Flexible Electronics, Northwestern Polytechnical University, 1 Dong Xiang Road, Xi'an 710072, P.R. China.

[§]College of Chemistry & Chemical Engineering, Hubei University, 368 You Yi Road, Wuhan 430062, P.R. China.

[‖]School of Science, MOE Key Laboratory of Material Physics and Chemistry Under Extraordinary Conditions, Ministry of Education, Northwestern Polytechnical University, 1 Dong Xiang Road, Xi'an, 710072, P.R. China.

[⊥]J.W. and T.C. contributed equally to this work.

[*]Author to whom correspondence should be addressed.

E-mail: iamcguan@nwpu.edu.cn (C. G.), cxpan@whu.edu.cn (C. P.)

Number of pages: 12

Number of figures: 7

Number of tables: 2

Experimental section

Material synthesis

Preparation of cobalt-based metal-organic frameworks (Co-MOFs) nanowall arrays on carbon cloth (CC). An aqueous solution contains $C_4H_6N_2$ (60 mL, 0.4 M) was quickly poured into the aqueous solution of $Co(NO_3)_2 \cdot 6H_2O$ (60 mL, 50 mM), after which a piece of acid-treated CC substrate (2.0 × 6.0 cm^2) was immersed into the mixture solution. After reaction for 4 h at 25 °C, the sample was taken out, cleaned with deionized water and dried overnight.

Preparation of heterogeneous WS_2/CoS_2 arrays on CC. A piece of Co-MOFs/CC (2.0 × 1.5 cm^2) was immersed into an ethanol/water solution (4:1 in volume, 100 mL) containing Na_2WO_4 (0.2 g) at 85 °C. After the purple colour of the Co-MOFs disappeared (~15 min), the sample was taken out, washed with ethanol repeatedly, and dried at 60 °C. Then the as-prepared sample was placed in the center of a horizontal-tube furnace. 1.0 g of sulfur powders was placed at the upstream position 15 cm away from the center. After annealing the as-prepared sample at 500 °C for 2 h with a heating rate of 10 °C min^{-1} under Ar with a flow rate of 40 mL min^{-1}, $WS_2/CoS_2/CC$ was obtained. The mass loading of WS_2/CoS_2 is ~2.0 mg cm^{-2}.

Preparation of hollow CoS_2 arrays on CC. A piece of Co-MOFs/CC (2.0 × 1.5 cm^2) was immersed into an ethanol/water solution (4:1 in volume, 100 mL) at 85 °C. After the purple colour of the Co-MOFs disappeared (~10 min), the sample was taken out, washed with ethanol repeatedly, and dried at 60 °C. Then the as-prepared sample was placed in the center of a horizontal-tube furnace. 1.0 g of sulfur powders was

placed at the upstream position 15 cm away from the center. After annealing the as-prepared sample at 500 °C for 2 h with a heating rate of 10 °C min^{-1} under Ar with a flow rate of 40 mL min^{-1}, CoS_2/CC was obtained. The mass loading of CoS_2 is ~1.5 mg cm^{-2}.

Preparation of Pt/C on CC: commercial Pt/C (20 wt %, Alfa Aesar) was well-dispersed in diluted Nafion alcohol solution (0.5 mL of ethanol and 50 μL of Nafion) to form a homogeneous suspension. Then the suspension was drop casted onto CC and drying at room temperature.

Characterization

The morphology, microscopic structure and chemical composition of the samples were characterized by field emission scanning electron microscopy (FESEM, FEI, Verios G4), transmission electron microscopy (TEM, FEI, FEI Talos F200X TEM), X-ray diffraction (XRD, Bruker Axs, XD-3), and X-ray photoelectron spectroscopy (XPS, Kratos, Axis Supra), respectively.

Electrochemical measurement

Electrochemical measurements were taken on a CHI 660e electrochemistry workstation at room temperature. The HER catalytic activities of the samples were tested in a conventional three-electrode system. 0.5 M H_2SO_4, 1.0 M PBS, and 1.0 M KOH solutions purged with N_2 were used as the acidic, neutral, and alkaline electrolytes, respectively. Catalysts on CC were directly used as the working electrode and a graphite rod was used as the counter electrode. An AgCl, a saturated calomel electrode (SCE), and an Hg/HgO were used as the reference electrode in 0.5 M H_2SO_4,

1.0 M PBS, and 1.0 M KOH solutions, respectively.

The linear sweep voltammogram (LSV) curves were measured at 2 mV s^{-1} with an iR corrected. All the measured potentials were referred to reversible hydrogen electrode (RHE) using the following equations: E(RHE) = E(AgCl) + 0.0592 × pH + 0.2046 (Equation S1), E(RHE) = E(SCE) + 0.0592 × pH + 0.244 (Equation S2), and E(RHE) = E(Hg/HgO) + 0.0592 × pH + 0.098 (Equation S3). The Tafel plots were calculated by the Tafel equation, $\eta = b \log j + a$ (Equation S4), where b is the Tafel slope, j is the current density, and a is the intercept relative to the exchange current density. The accelerated degradation tests were measured through continuous CV measurements in the potential range from -155 mV to 45 mV (vs RHE in 0.5 M H_2SO_4), -190 mV to 10 mV (vs RHE in 1.0 M PBS) and -130 mV to 70 mV (vs RHE in 1.0 M KOH) with a scan rate of 100 mV s^{-1} for 1000 cycles. The HER stability was determined by a chronopotentiometry measurement at a current density of 10 mA cm^{-2} for 24 h without any iR-drop compensation. What's more, the electrochemical impedance spectroscopy (EIS) measurements were performed by applying an AC voltage with 5 mV amplitude in a frequency range from 0.01 Hz to 100 kHz at open circuit voltage which was chosed the potential at 10 mA cm^{-2} of LSV curves. The electrochemical double-layer capacitance (C_{dl}) was determined from the Cyclic Voltammetry (CV) curves measured in a potential range without redox process by $C_{dl} = I / \nu$ (Equation S5), where I (mA cm^{-2}) is the charging current and ν (mV s^{-1}) is the scan rate. CV curves of various samples were recorded from 0.51 to 0.61 V (vs RHE in 0.5 M H_2SO_4), 0.56 to 0.66 V (vs RHE in 1.0 M PBS) and 0.63 to 0.73 V (vs RHE

in 1.0 M KOH) with scan rates of 10, 20, 30, 40, and 50 mV s^{-1}. The electrochemically active surface area (ECSA) was estimated from the electrochemical C_{dl}. The specific capacitance (C_s) value C_s = 0.040 mF cm^{-2} is adopted for the estimation of ECSA. The ECSA of WS_2/CoS_2/CC and CoS_2/CC can be calculated as below: ECSA = $C_{dl\text{-}catalyst}$ / C_s (Equation S6). All the potentials in the text, if not specified, were recorded relative to the RHE and the current density was normalized to the geometrical surface area.

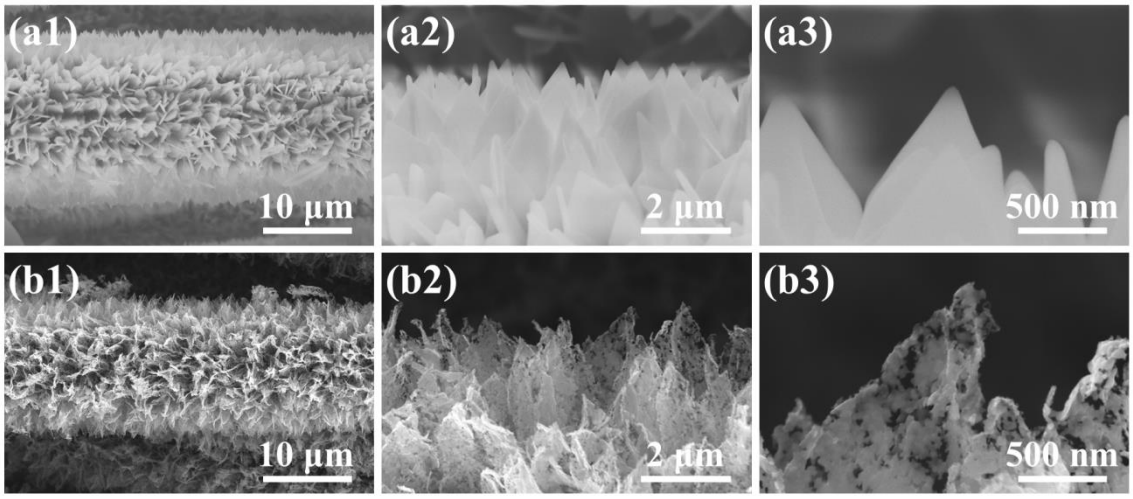

Figure S1. SEM images of (a1-a3) Co-MOF/CC and (b1-b3) CoS_2/CC.

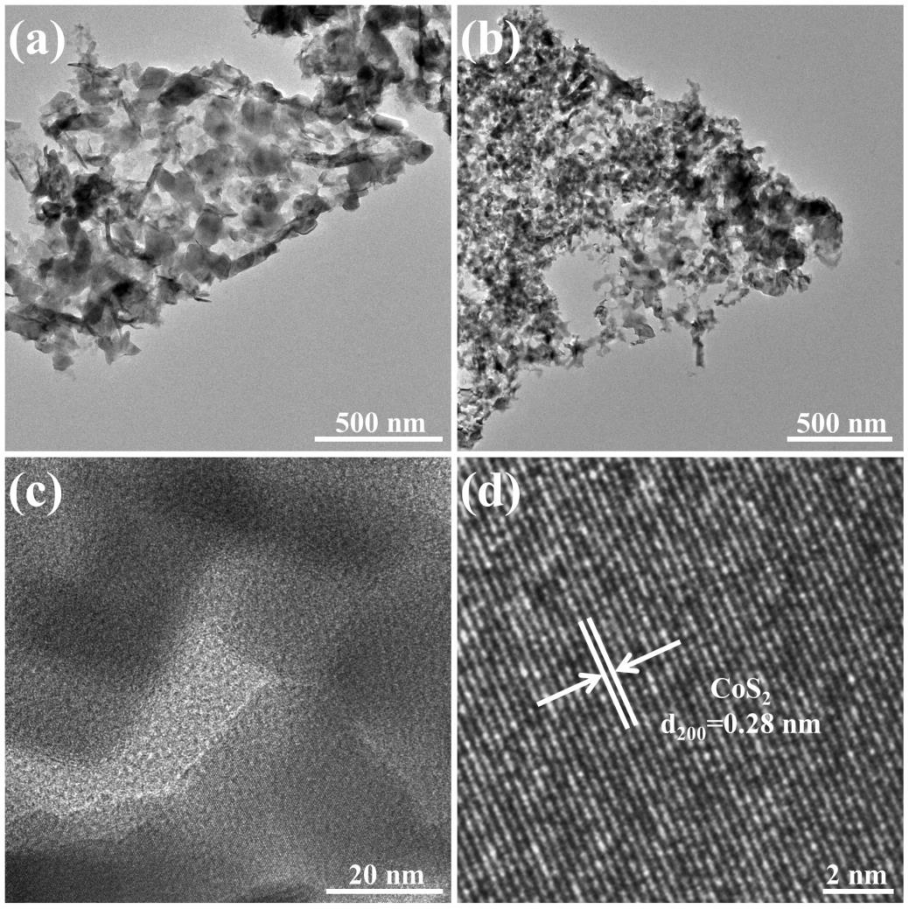

Figure S2. (a) TEM image of WS_2/CoS_2 heterostructure. (b-d) TEM andcorresponding high resolution TEM images of pure CoS_2.

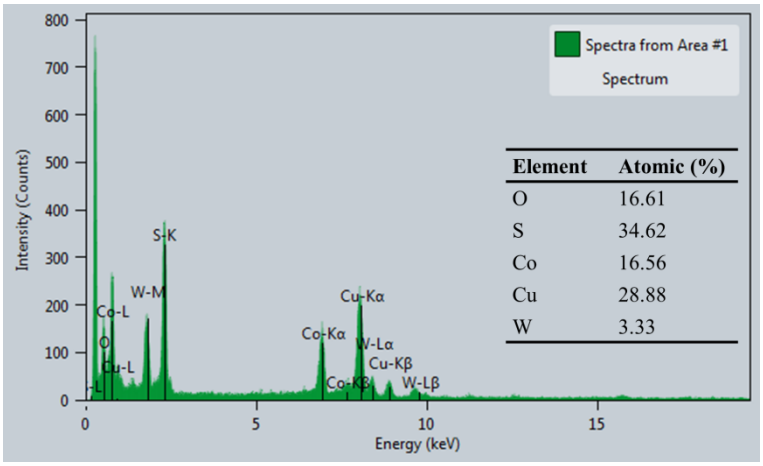

Figure S3. EDS spectrum and atomic ratios (Inset) of the WS_2/CoS_2 heterostructure.

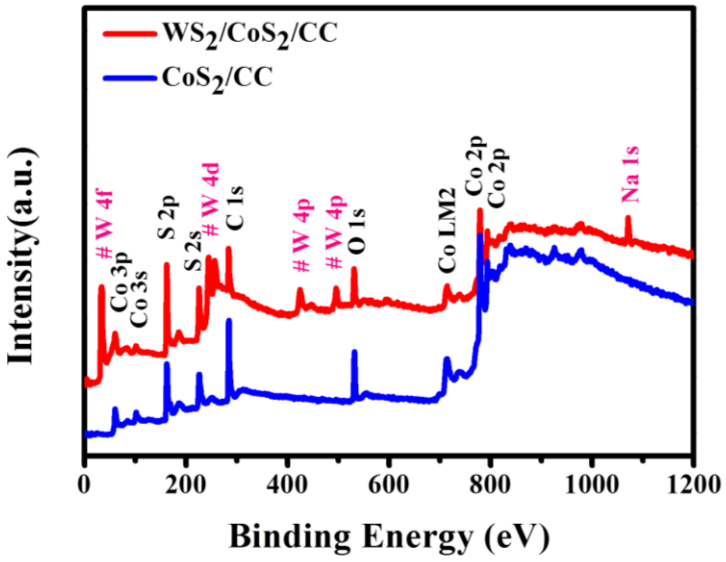

Figure S4. XPS survey spectra of $WS_2/CoS_2/CC$ and CoS_2/CC.

Table S1. HER performances comparison of recently reported heterostructures in different electrolytes.

Catalysts	Overpotential @ 10 mA cm^{-2} (mV)	Eletrolytes	References
$NiCo_2O_4$/CuS	72.3	0.5 M H_2SO_4	[1]
MoSSe@rGO	153	0.5 M H_2SO_4	[2]
MoS_2/Ni_3S_2	110	1.0 M KOH	[3]
Ni_2P/CoP	55	0.5 M H_2SO_4	[4]
$W_xC@WS_2$	146	0.5 M H_2SO_4	[5]
$Co_3S_4@MoS_2$	210	0.5 M H_2SO_4	[6]
$Ni(OH)_2/MoS_2$	80	1.0 M KOH	[7]
$MoS_2/Fe_5Ni_4S_8$	120	1.0 M KOH	[8]
NiFe LDH@NiCoP	120	1.0 M KOH	[9]
WS_2-CoS_2	245	0.5 M H_2SO_4	[10]
Co_9S_8/Ni_3S_2	128	1.0 M KOH	[11]
MoS_2/CoS_2	90 85 150	0.5 M H_2SO_4 1.0 M KOH 1.0 M PBS	[12]
$Mo_2C@MoS_2$	67 121 86	0.5 M H_2SO_4 1.0 M PBS 1.0 M KOH	[13]
Mo_2C/VC	122	0.5 M H_2SO_4	[14]
$MoSe_2/MoS_2$	162	0.5 M H_2SO_4	[15]
WS_2/CoS_2	**146** **175** **122**	**0.5 M H_2SO_4** **1.0 M PBS** **1.0 M KOH**	**In this work**

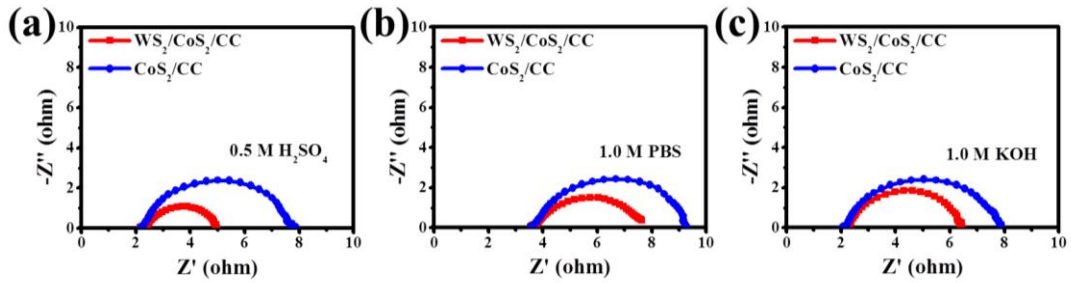

Figure S5. Nyquist plots of $WS_2/CoS_2/CC$ and CoS_2/CC in (a) 0.5 M H_2SO_4, (b) 1.0 M PBS, (c) 1.0 M KOH.

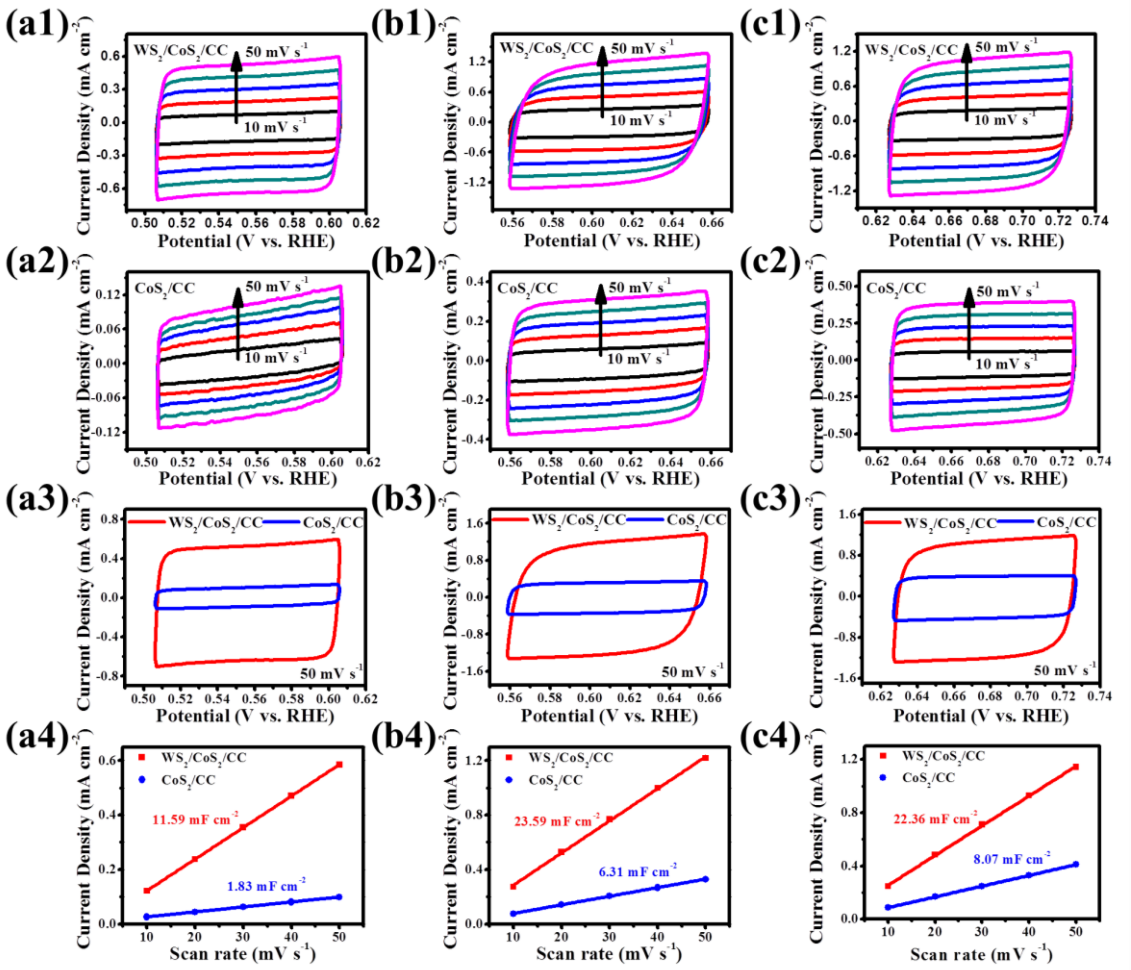

Figure S6. CV and C_{dl} curves of $WS_2/CoS_2/CC$ and CoS_2/CC in (a1-a4) 0.5 M H_2SO_4, (b1-b4) 1.0 M PBS, (c1-c4) 1.0 M KOH.

Table S2. The electrochemically active surface area (ECSA) calculated from C_{dl} of WS_2/CoS_2/CC and CoS_2/CC in different electrolytes.

Catalysts	0.5 M H_2SO_4	1.0 M PBS	1.0 M KOH
WS_2/CoS_2/CC	289.75 cm^2	589.75 cm^2	559.00 cm^2
CoS_2/CC	45.75 cm^2	157.75 cm^2	201.75 cm^2

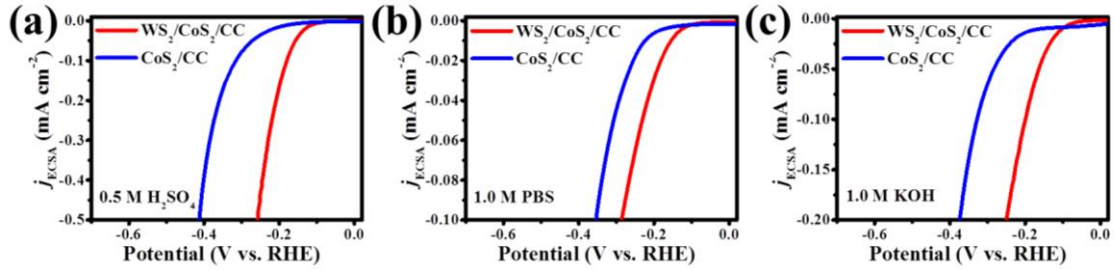

Figure S7. IR-compensated polarization curves of WS_2/CoS_2/CC and CoS_2/CC after normalizing the geometric current densities to the corresponding ECSA in (a) 0.5 M H_2SO_4, (b) 1.0 M PBS, and (c) 1.0 M KOH, respectively.

References

1. An, L.; Huang, L.; Zhou, P.; Yin, J.; Liu, H.; Xi, P. A Self-Standing High-Performance Hydrogen Evolution Electrode with Nanostructured $NiCo_2O_4$/CuS Heterostructures. *Adv. Funct. Mater.* **2015,** *25*, 6814-6822, DOI 10.1002/adfm.201503784.

2. Konkena, B.; Masa, J.; Xia, W.; Muhler, M.; Schuhmann, W. MoSSe@reduced graphene oxide nanocomposite heterostructures as efficient and stable electrocatalysts for the hydrogen evolution reaction. *Nano Energy* **2016,** *29*, 46-53, DOI 10.1016/j.nanoen.2016.04.018.

3. Zhang, J.; Wang, T.; Pohl, D.; Rellinghaus, B.; Dong, R.; Liu, S.; Zhuang, X.; Feng, X. Interface Engineering of MoS_2/Ni_3S_2 Heterostructures for Highly Enhanced Electrochemical Overall-Water-Splitting Activity. *Angew. Chem. Int. Ed.* **2016,** *55*,

6702-6707, DOI 10.1002/anie.201602237.

4. Tang, W.; Wang, J.; Guo, L.; Teng, X.; Meyer, T. J.; Chen, Z. Heterostructured Arrays of $Ni_xP/S/Se$ Nanosheets on CoxP/S/Se Nanowires for Efficient Hydrogen Evolution. *ACS Appl. Mater. Interfaces* **2017,** *9*, 41347-41353, DOI 10.1021/acsami.7b14466.

5. Wang, F.; He, P.; Li, Y.; Shifa, T. A.; Deng, Y.; Liu, K.; Wang, Q.; Wang, F.; Wen, Y.; Wang, Z.; Zhan, X.; Sun, L.; He, J. Interface Engineered $W_xC@WS_2$ Nanostructure for Enhanced Hydrogen Evolution Catalysis. *Adv. Funct. Mater.* **2017,** *27*, 1605802, DOI 10.1002/adfm.201605802.

6. Guo, Y.; Tang, J.; Qian, H.; Wang, Z.; Yamauchi, Y. One-Pot Synthesis of Zeolitic Imidazolate Framework 67-Derived Hollow $Co_3S_4@MoS_2$ Heterostructures as Efficient Bifunctional Catalysts. *Chem. Mater.* **2017,** *29*, 5566-5573, DOI 10.1021/acs.chemmater.7b00867.

7. Zhang, B.; Liu, J.; Wang, J.; Ruan, Y.; Ji, X.; Xu, K.; Chen, C.; Wan, H.; Miao, L.; Jiang, J. Interface engineering: The $Ni(OH)_2/MoS_2$ heterostructure for highly efficient alkaline hydrogen evolution. *Nano Energy* **2017,** *37*, 74-80, DOI 10.1016/j.nanoen.2017.05.011.

8. Wu, Y.; Li, F.; Chen, W.; Xiang, Q.; Ma, Y.; Zhu, H.; Tao, P.; Song, C.; Shang, W.; Deng, T.; Wu, J. Coupling Interface Constructions of $MoS_2/Fe_5Ni_4S_8$ Heterostructures for Efficient Electrochemical Water Splitting. *Adv. Mater.* **2018,** *30*, 803151, DOI 10.1002/adma.201803151.

9. Zhang, H.; Li, X.; Hähnel, A.; Naumann, V.; Lin, C.; Azimi, S.; Schweizer, S. L.;

Maijenburg, A. W.; Wehrspohn, R. B. Bifunctional Heterostructure Assembly of NiFe LDH Nanosheets on NiCoP Nanowires for Highly Efficient and Stable Overall Water Splitting. *Adv. Funct. Mater.* **2018,** *28*, 1706847, DOI 10.1002/adfm.201706847.

10. Jing, Y.; Mu, X.; Xie, C.; Liu, H.; Yan, R.; Dai, H.; Liu, C.; Zhang, X.-D. Enhanced hydrogen evolution reaction of WS_2-CoS_2 heterostructure by synergistic effect. *Int. J. Hydrogen Energy* **2019,** *44*, 809-818, DOI 10.1016/j.ijhydene.2018.11.012.

11. Du, F.; Shi, L.; Zhang, Y.; Li, T.; Wang, J.; Wen, G.; Alsaedi, A.; Hayat, T.; Zhou, Y.; Zou, Z. Foam-like Co_9S_8/Ni_3S_2 heterostructure nanowire arrays for efficient bifunctional overall water-splitting. *Appl. Catal. B: Environ.* **2019,** *253*, 246-252, DOI 10.1016/j.apcatb.2019.04.067.

12. Tang, B.; Yu, Z. G.; Zhang, Y.; Tang, C.; Seng, H. L.; Seh, Z. W.; Zhang, Y.-W.; Pennycook, S. J.; Gong, H.; Yang, W. Metal-organic framework-derived hierarchical MoS_2/CoS_2 nanotube arrays as pH-universal electrocatalysts for efficient hydrogen evolution. *J. Mater. Chem. A* **2019,** *7*, 13339-13346, DOI 10.1039/c9ta00545e.

13. Yang, S.; Wang, Y.; Zhang, H.; Zhang, Y.; Liu, L.; Fang, L.; Yang, X.; Gu, X.; Wang, Y. Unique three-dimensional $Mo_2C@MoS_2$ heterojunction nanostructure with S vacancies as outstanding all-pH range electrocatalyst for hydrogen evolution. *J. Catal.* **2019,** *371*, 20-26, DOI 10.1016/j.jcat.2019.01.020.

14. Huang, C.; Miao, X.; Pi, C.; Gao, B.; Zhang, X.; Qin, P.; Huo, K.; Peng, X.; Chu, P. K. Mo_2C/VC heterojunction embedded in graphitic carbon network: An advanced electrocatalyst for hydrogen evolution. *Nano Energy* **2019,** *60*, 520-526, DOI

10.1016/j.nanoen.2019.03.088.

15. Li, S.; Zang, W.; Liu, X.; Pennycook, S. J.; Kou, Z.; Yang, C.; Guan, C.; Wang, J. Heterojunction engineering of $MoSe_2/MoS_2$ with electronic modulation towards synergetic hydrogen evolution reaction and supercapacitance performance. *Chem. Eng. J.* **2019,** *359*, 1419-1426, DOI 10.1016/j.cej.2018.11.036.